Supporting Information

Synthesis, Two-Dimensional Assembly and Surface Pressure Induced Coalescence of Ultra Narrow PbS Nanowires

Israel Patla[1], Somobrata Acharya[2#], Leila Zeiri[1], Jacob Israelachvili[3], Shlomo Efrima[1] and Yuval Golan[2]*

[1]Department of Chemistry, [2]Department of Materials Engineering, and the Ilse Katz Center for Meso and Nanoscale Science and Technology, Ben-Gurion University of the Negev, Beer Sheva 84105, Israel [3]Department of Chemical Engineering, Materials Department and Materials Research Laboratory, University of California, Santa Barbara, CA 93106, USA.

 # Present address: International Center for Young Scientists, National Research Institute for Materials Science, 1-1 Namiki Tsukuba, Ibaraki 305-0044, JAPAN

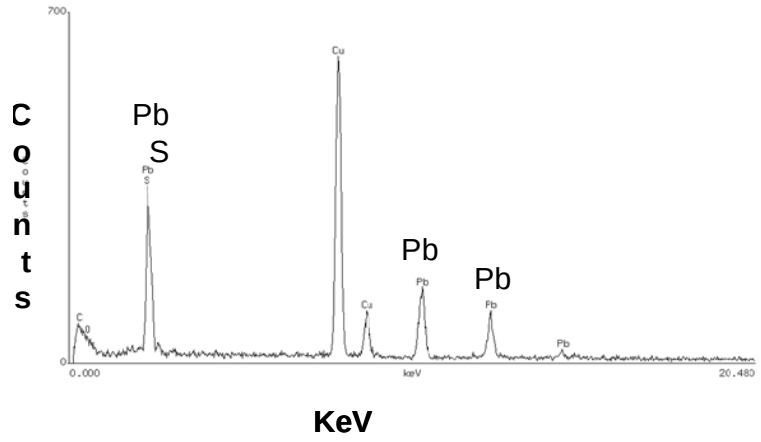

Elements	Wires	
	Pb	S
Atom %	47	53
Weight %	85	15

Figure S1. Energy dispersive spectroscopy (EDS) elemental analysis spectra of PbS wires taken in the TEM. The table lists the atom and weight percentage of Pb and S obtained for the wires.

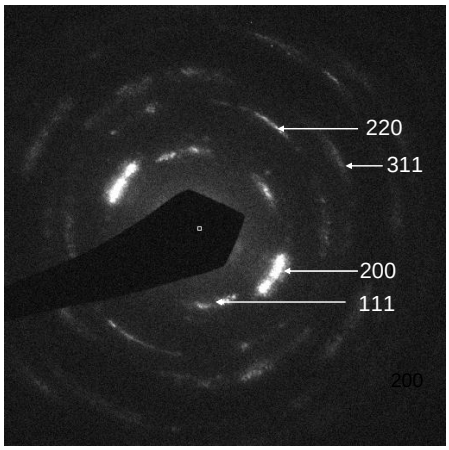

Figure S2. The SAED patterns obtained from the PbS wires (see Figure 1a) shows the rock salt cubic structure with 111, 200, 220, and 311 diffraction rings, in line with the inter-planer distances of 0.342 nm, 0.2969, 2.099 and 1.790 nm of PbS bulk rock salt structure (JCPDS 05-0592). The interplanar distance 0.29±0.03 nm observed in HRTEM (Figure 1b) corresponds to the (200) plane of PbS rock salt structure. The strongest intensity of the 200 reflection indicates a preferred orientation in which the wires are oriented with the [100] crystallographic axis parallel to the long axis of the wire. The zone axis for the SAED pattern is $[01\bar{1}]$ in which both the (200) and (111) planes are in diffraction conditions.

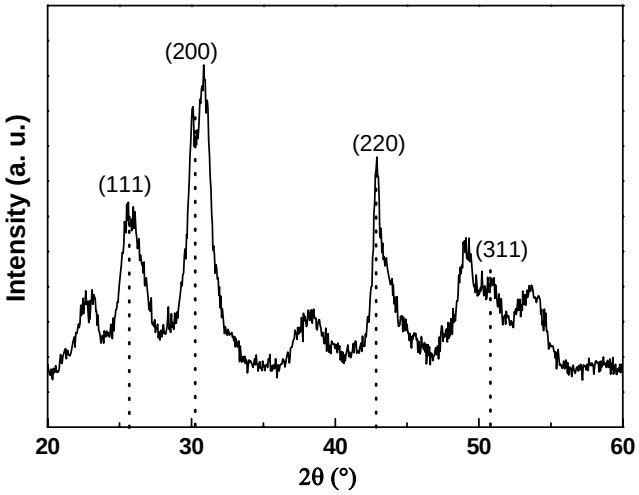

Figure S3. The XRD of powder samples of PbS wires matches well to the standard rocksalt structure of PbS ($Fm\bar{3}m$, a_0 = 5.9362Å). The 200 diffraction peak of the nanocrystals is strongest, as expected for powder rocksalt specimen. The dotted lines denote the literature values for rocksalt PbS according to JCPDS #05-0592.

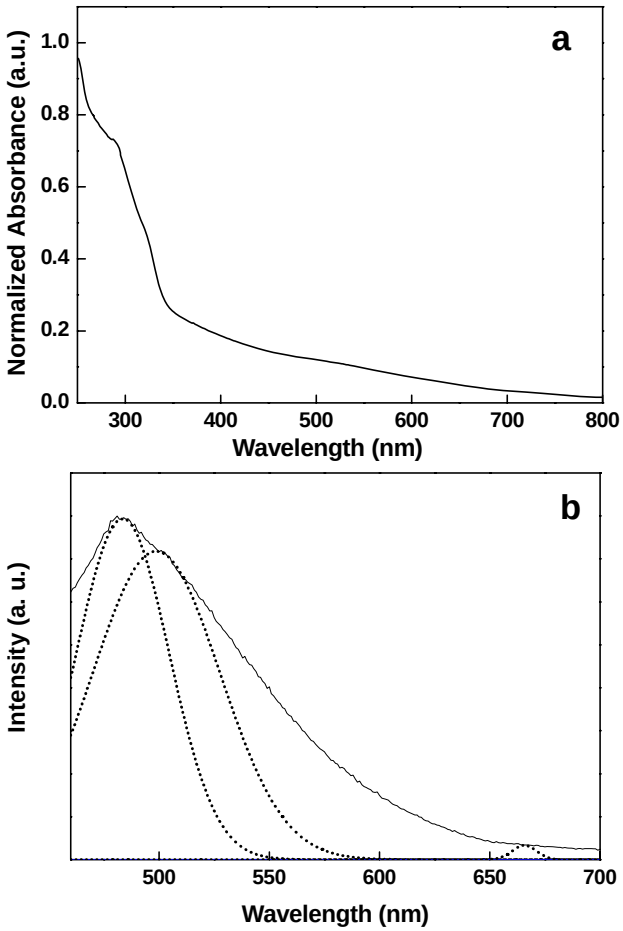

Figure S4. The room temperature (a) absorption and (b) PL spectra of PbS nanowire suspension in dichloromethane. The absorption spectrum shows three bands at 520 nm (2.39 eV), 325 nm (3.83 eV) and 290 nm (4.29 eV). All these bands are due to exciton absorption corresponding to the $1S_c \leftarrow 1S_h$, $1S_c \leftarrow 1P_h$, $1P_c \leftarrow 1P_h$ transitions, respectively. The appearance of these three excitonic peaks and the overall blue shifting in comparison to bulk PbS as well as to other reported PbS nanoparticles reflects the uniformity and defect-free structure of the wires, with less surface traps for electron-hole pairs. The PL spectrum shows a strong band edge emission at 480 nm (2.87 eV) with FWHM of 45 nm. De-convolution (dotted curves) of the spectrum reveals a shoulder at 500 nm and a low energy very weak peak at 665 nm. The overall blue shift in the optical spectra is likely to result from the very strong quantum confinement effect, namely the ultra-narrow width of the wires.

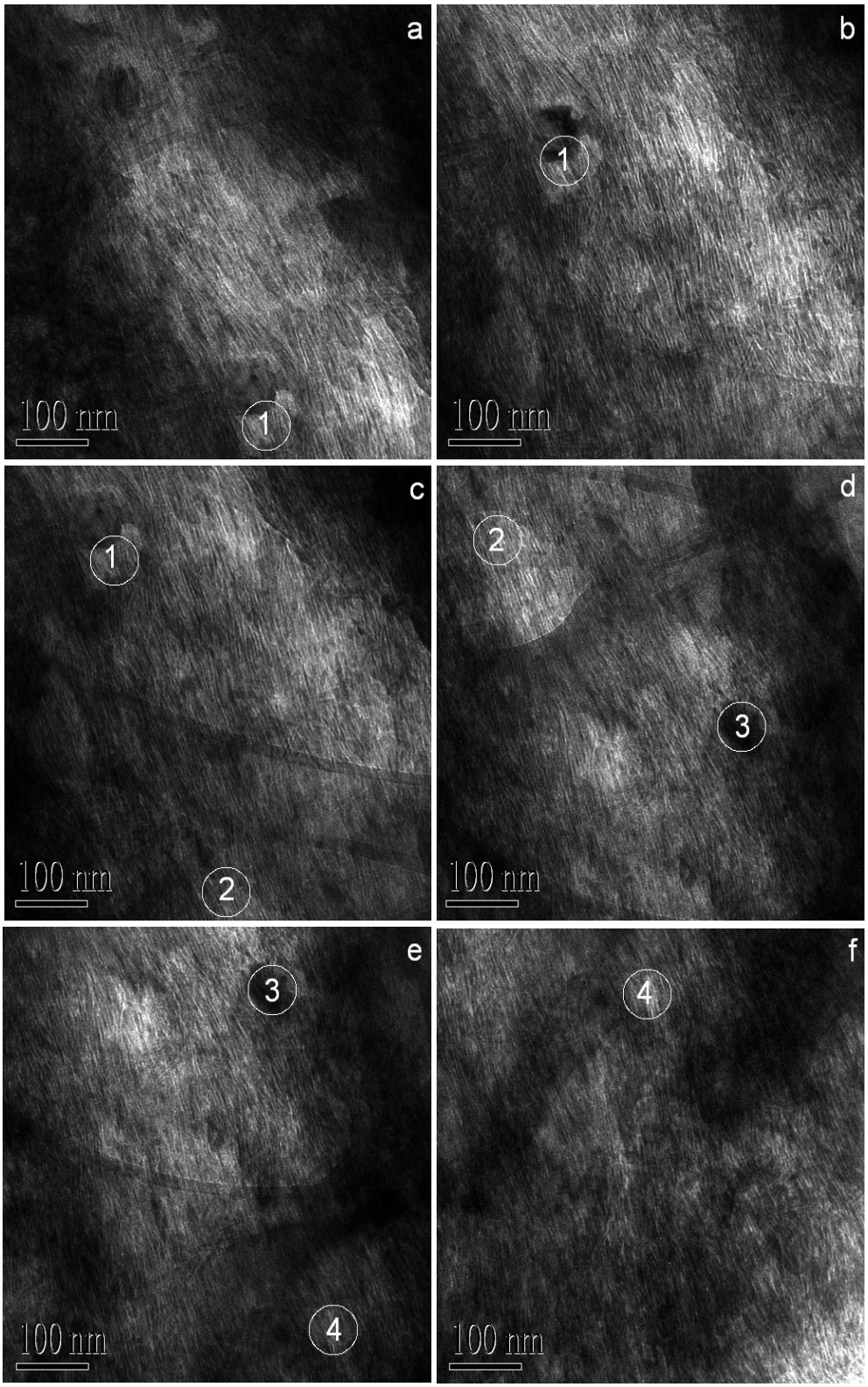
a
100 nm
1
b
1
100 nm
c
1
100 nm
2
d
2
3
100 nm
e
3
100 nm
4
f
4
100 nm

Figure S5. A composite map comprised of large area TEM images showing the aligned parallel nanowires following transfer onto a TEM grid using the Langmuir Blodgett method. The monolayer of the aligned nanowires was lifted at Π=23 mN/m and T=22ºC. Images a-f represent a continuous area in the TEM grid with the representative location marks indicated by the circled numbers. The area represented here is over 3 μm^2, which is only part of the total aligned area of ca. 15 μm^2. Such long range areas are observed frequently in many different regions of the TEM grid. The nanowires retain the same width after alignment with average diameter oϕ 1.8±0.08 nm and pitch of 2.7±0.08 nm.

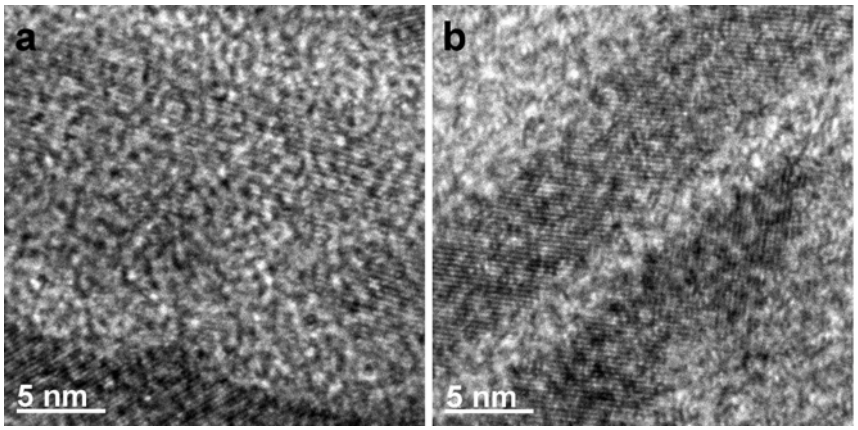

Figure S6. HRTEM images showing the single crystal nature of the coalesced nanowires. Note that the different planes (d-spacings) observed in the lattice images are determined by the defocus value *and* by the sample thickness**.**